



The Microstructure and Electronic Properties of Yttrium Oxide Doped With Cerium: A Theoretical Insight

Meng Ju^{1,2}, Jingjing Wang^{2*}, Jing Huang¹, Chuanzhao Zhang^{3*}, Yuanyuan Jin³, Weiguo Sun⁴, Shichang Li⁵ and Yunhong Chen²

¹ School of Physical Science and Technology, Southwest University, Chongqing, China, ² College of Computer and Information Engineering, Hubei Normal University, Huangshi, China, ³ Department of Physics and Optoelectronic Engineering, Yangtze University, Jingzhou, China, ⁴ Centre for Science at Extreme Conditions and School of Physics and Astronomy, Scottish Universities Physics Alliance (SUPA), University of Edinburgh, Edinburgh, United Kingdom, ⁵ School of Science, Chongqing University of Posts and Telecommunications, Chongqing, China

OPEN ACCESS

Edited by:

Zhenxiang Cheng,
University of Wollongong, Australia

Reviewed by:

Li Zhu,
Carnegie Institution for Science (CIS),
United States

Hui Li,
Temple University, United States

*Correspondence:

Jingjing Wang
scu_wjj@163.com
Chuanzhao Zhang
zcz19870517@163.com

Specialty section:

This article was submitted to
Theoretical and Computational
Chemistry,
a section of the journal
Frontiers in Chemistry

Received: 05 March 2020

Accepted: 01 April 2020

Published: 28 April 2020

Citation:

Ju M, Wang J, Huang J, Zhang C,
Jin Y, Sun W, Li S and Chen Y (2020)
The Microstructure and Electronic
Properties of Yttrium Oxide Doped
With Cerium: A Theoretical Insight.
Front. Chem. 8:338.
doi: 10.3389/fchem.2020.00338

Trivalent Cerium (Ce³⁺) doped Yttrium Oxide (Y₂O₃) host crystal has drawn considerable interest due to its popular optical 5d-4f transition. The outstanding optical properties of Y₂O₃:Ce system have been demonstrated by previous studies but the microstructures still remain unclear. The lacks of Y₂O₃:Ce microstructures could constitute a problem to further exploit its potential applications. In this sense, we have comprehensively investigated the structural evolutions of Y₂O₃:Ce crystals based on the CALYPSO structure search method in conjunction with density functional theory calculations. Our result uncovers a new rhombohedral phase of Y₂O₃:Ce with R-3 group symmetry. In the host crystal, the Y³⁺ ion at central site can be naturally replaced by the doped Ce³⁺, resulting in a perfect cage-like configuration. We find an interesting phase transition that the crystallographic symmetry of Y₂O₃ changes from cubic to rhombohedral when the impurity Ce³⁺ is doped into the host crystal. With the nominal concentration of Ce³⁺ at 3.125%, many metastable structures are also identified due to the different occupying points in the host crystal. The X-ray diffraction patterns of Y₂O₃:Ce are simulated and the theoretical result is comparable to experimental data, thus demonstrating the validity of the lowest energy structure. The result of phonon dispersions shows that the ground state structure is dynamically stable. The analysis of electronic properties indicate that the Y₂O₃:Ce possesses a band gap of 4.20 eV which suggests that the incorporation of impurity Ce³⁺ ion into Y₂O₃ host crystal leads to an insulator to semiconductor transition. Meanwhile, the strong covalent bonds of O atoms in the crystal, which may greatly contribute to the stability of ground state structure, are evidenced by electron localization function. These obtained results elucidate the structural and bonding characters of Y₂O₃:Ce and could also provide useful insights for understanding the experimental phenomena.

Keywords: crystal structure prediction (CSP), electronic properties, structural evolution, rare earth element, theoretical calculation DFT

INTRODUCTION

The rare-earth Cerium ions doped crystals constitute an attractive class of materials that have been extensively used in many kinds of fields including scintillation phosphors, laser medium, and white light emitting diode phosphors (Han et al., 2019; Lin et al., 2019; Masanori et al., 2020). The outstanding optical behaviors of trivalent Cerium ion (Ce³⁺) has drawn considerable interest due to its popular optical 5d-4f transition. Among various host materials, Yttrium Oxide (Y₂O₃) crystal is considered to be the most promising sesquioxide host because of its unique chemical and thermal stability. The Y₂O₃ host crystal is also one of the multifunctional materials that can give rise to many application areas owing to its fabulous capacity of incorporating the activated laser ions (Ming et al., 2018; Wang et al., 2018; Ju et al., 2020). The latest study has indicated that the Ce³⁺ doped Y₂O₃ crystals (Y₂O₃:Ce) exhibit dominant emission bands at around 380 nm and relatively low intensive band at 560 nm (Gieszczyk et al., 2019). The results further demonstrate the ideal applications of energy storage phosphors for Y₂O₃:Ce. The excellent advantages of Y₂O₃:Ce can also be evidenced by the effective use as various laser ceramics (Lupei et al., 2017).

It is well-known that the laser actions can be generally identified in the absorption and emission spectra of rare-earth doped materials. In order to explore the luminescent properties of Y₂O₃:Ce, Jia et al. (2001) had synthesized the Y₂O₃:Ce nanoparticles in experiments and measured the photoluminescence spectra at room temperature. Their results revealed that the strong emissions cover the ultraviolet band from 240 nm to 380 nm. To explain the emission lines of the spectra, Loitongbam et al. (2013) measured the luminescence intensities of Y₂O₃:Ce and found that the characteristic blue color emissions at 424 and 486 nm are originated from Ce³⁺ ion 5d (spectra terms) → 4f (spectra terms). An unexpected optical activity, including up and down conversions, for Y₂O₃:Ce crystal was firstly observed by Marin et al. (2013). Although the laser actions were established by a few studies, many researchers were motivated to probe the structural properties of Y₂O₃:Ce. The effect of doping Ce³⁺ ion into Y₂O₃ fibers was investigated by Zhu et al. (2008). They found that the obvious quenching of the luminescence occurred at Ce³⁺ concentration of 5%. By using the solid-state-reactive method, Liu et al. (2020) carried out a study on the structures of a series of Ce³⁺ doped Y₂O₃ ternary ceramics. The results demonstrated that the solubility of Ce³⁺ concentration at 4% could broaden emission spectra and lead to a large red-shift, which is attractive for the white light emitting. A recent research on the structural properties of Y₂O₃:Ce was conducted by Krutikova et al. (2020). The nanopowders were obtained by laser ablation and the X-ray diffraction (XRD) patterns of Y₂O₃:Ce crystal were reported. By looking at the investigations concerning Y₂O₃:Ce in the literatures, it can be concluded that the systematic electronic structures have not yet been explored, especially for the theoretical insights. Furthermore, the lacks of Y₂O₃:Ce microstructures constitute a problem to exploit its potential prospects in many applications.

In this paper, we have performed a systematic study on the stable structures and electronic properties for Y₂O₃ doped

with Ce³⁺ system. By using the CALYPSO (Crystal structure AnaLYsis by Particle Swarm Optimization) structure search method (Wang et al., 2010, 2012; Li et al., 2014) combined with first-principle calculation, the low-lying energy structures of Y₂O₃:Ce are extensively searched. A large number of candidate structures are obtained and the ground state structure together with the first four metastable structures is analyzed in detail. Based on the obtained lowest energy structure of Y₂O₃:Ce, we thoroughly conduct a calculation of the electronic properties, which could provide powerful guidance for further experimental and theoretical studies.

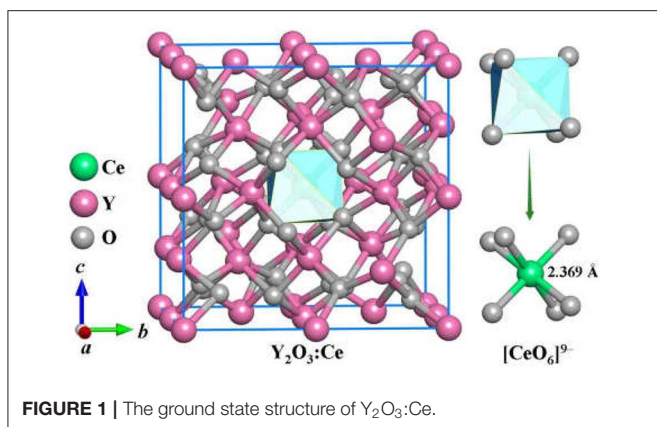
COMPUTATIONAL DETAILS

We have carried out an unbiased structure search for Y₂O₃ doped with Ce³⁺ system based on the CALYPSO method (Wang et al., 2010, 2012; Li et al., 2014). The CALYPSO is able to successfully predict the stable structures only with given chemical composition of the system (Lu et al., 2013, 2017, 2018; Lu and Chen, 2018). The detailed method of CALYPSO has been reported in many papers (Ju et al., 2016, 2017, 2019a,b). In this work, the structure searches are performed for Y₂O₃ doped with Ce system at 80 atoms in one unit cell. The obtained low-lying energy structures are used to perform further geometric optimizations. We conduct the *ab initio* structural relaxations and electronic properties calculations in the framework of density functional theory (DFT) by using the local density approximation (LDA) exchange correlation functional, as implemented in the Vienna Ab Initio Simulation Package (VASP) (Kresse and Hafner, 1993; Kresse and Furthmuller, 1996; Perdew et al., 1996). Considering the strong f-electrons correlations within the heavy Ce³⁺ ion, an onsite Coulomb repulsion $U = 5.0$ eV is employed in the calculations (Herbst and Waston, 1978). We use the projector-augmented wave method to simulate the valence electron space of Ce, Y, and O atoms. The used electrons are 4f¹5s²5p⁶5d¹6s², 4s²4p⁶4d¹5s², and 2s²2p⁴, respectively. Sufficiently fine Monkhorst-Pack k meshes and 500 eV cutoff energy have been chosen to make sure that the calculated enthalpy of each atom is <1 meV. By using a super cell approach, the phonon dispersion spectra are calculated in PHONOPY code (Atsushi et al., 1993). The electron localization function (ELF) (Becke and Edgecombe, 1990; Savin et al., 1992) analysis of Y₂O₃:Ce is performed and the results are depicted in the VESTA software (Momma and Izumi, 2011). The projected Crystal Orbital Hamilton Population (COHP) (Richard and Peter, 1993) are calculated by the LOBSTER code (Volker et al., 2011; Stefan et al., 2016).

RESULTS AND DISCUSSIONS

Crystal Structures

The stable structures for Y₂O₃:Ce system are favorably identified by using the method described in section Computational Details. On the basis of total energies from low to high, we have plotted the lowest-energy structure of Y₂O₃:Ce in **Figure 1**, together with the local [CeO₆]⁹⁻ complex ligand. Noticeably, the ground



state structure of Y₂O₃:Ce possesses a novel structure with R-3 (No. 148) space group. To the best of our knowledge, the rhombohedral phase of Y₂O₃:Ce crystal is uncovered for the first time. This result indicates an interesting phase transition that the crystallographic symmetry of Y₂O₃ changes from cubic (Ia-3) to rhombohedral (R-3) when the impurity Ce³⁺ is doped into the host crystal. It is clearly seen from **Figure 1** that the host Y³⁺ ion can be naturally occupied by the impurity Ce³⁺ ion. Interestingly, the Wyckoff position of Ce³⁺ is 1b (0.5, 0.5, 0.5), suggesting that the ground state Y₂O₃:Ce is a standard cage-like structure. This result is different from that of Y₂O₃:Nd system (Ju et al., 2020). For reference, the coordinates of all atoms for the ground state Y₂O₃:Ce are summarized in **Table 1**. The estimated unit cell parameters and volume for Y₂O₃:Ce are $a = b = c = 10.541$ Å and 1171.371 Å³ (Han et al., 2019), respectively. These values are slightly smaller than those of pure Y₂O₃ but are comparable to the results reported by Kumar et al. (2017). As regard to the local structure, the Ce³⁺ ion is calculated to be 6-fold coordinated by O²⁻, forming the [CeO₆]⁹⁻ complex ligand. The cationic site symmetry of Ce³⁺ is C_{3i} with six equal Ce–O bonds of 2.369 Å. This bond length is similar with that of Y–O bonds because the effective radius of Ce³⁺ (1.03 Å) is very close to Y³⁺ (0.90 Å).

In the structure prediction, we adopt the chemical composition of Ce:Y:O = 1:31:48 to obtain the stable structures with nominal concentration of Ce³⁺. In this sense, the impurity Ce³⁺ in Y₂O₃ crystal is equal to 3.125 at %. Apart from the ground state structure, the CALYPSO also identifies a large number of candidate isomers that can be useful to study the structural evolution of the Y₂O₃:Ce. **Figure 2** illustrates the first four metastable structures of Y₂O₃:Ce. The isomer (a) has the same R-3 space group as the lowest energy structure while the impurity Ce³⁺ ions are likely to substitute the Y³⁺ at the lattice vertexes. The Ce³⁺ ion of isomer (a) takes the 1a (0, 0, 0) position. It is evidenced that the calculated crystal lattice parameters (10.543 Å) are nearly same as those of lowest-energy structure. The group symmetry of isomer (b) is predicted to be P1 with a triclinic phase. The Wyckoff position of Ce³⁺ is predicted to be 1a (0.25, 0.75, 0.25). Calculated result reveals that the isomer (c) exhibits a monoclinic structure which belongs to P2 symmetry. The impurity Ce³⁺ ion occupies the 1b (0, 0.47157,

TABLE 1 | Coordinates of all atoms for the ground state Y₂O₃:Ce.

Atom	x	y	z	Wyckoff site symmetry
Ce	0.50000	0.50000	0.50000	1b
Y1	0.50000	0	0	3d
Y4	0	0.50000	0.50000	3e
Y5	0	0	0	1a
Y8	1.21723	−0.00048	−0.24957	6f
Y9	0.78317	−0.50109	−0.24904	6f
Y10	0.28219	0.00104	0.25009	6f
Y11	0.72090	−0.50141	0.24728	6f
O1	0.64138	−0.12945	−0.09800	6f
O2	1.14358	−0.62871	0.40217	6f
O3	0.35267	−0.63253	0.60591	6f
O4	0.85797	−0.12919	0.09753	6f
O5	0.85966	0.12874	0.40167	6f
O6	0.35814	−0.37026	−0.09599	6f
O7	1.14102	−0.37007	0.09751	6f
O8	0.64188	0.12739	0.59868	6f

05) position. For the configuration of isomer (d), it is seen that the Ce³⁺ ions appear at the center sites of bottom and top in the crystal lattice. The isomer (d) is assigned to P1 group symmetry and is 0.27 eV energetically higher than ground state structure.

Although the X-ray powder diffraction (XRD) patterns of Y₂O₃:Ce crystals have been extensively studied, there appears to be inconsistencies of the spectra (Chien and Yu, 2008; Taibeche et al., 2016; Kumar et al., 2017). In order to clarify the crystal characters of the lowest-energy structure, we simulate the XRD patterns of Y₂O₃:Ce in the 2θ range of 15–65°. The result compared with experimental data is presented in **Figure 3**. It is evident that the calculated spectrum is in perfect agreement with the values measured by Kumar et al. (2017), demonstrating the validity of the lowest energy structure as well as the accuracy of our theoretical calculations. It should be pointed out that the simulated diffraction peak at 34° is ascribed to the (400) plane direction. This is accord with the result obtained by Taibeche et al. (2016) but different from the measured value proposed by Chien and Yu (2008). For comparison, the XRD patterns of the four isomers (a), (b), (c), and (d) are also provided in **Figure 3**. Although the overall distribution of the peaks in isomers is closely similar with each other, there are minor differences in the relative intensities. To evaluate the dynamical stability of Y₂O₃:Ce, the phonon spectrum within the Brillouin zone of ground state structure are calculated. **Figure 4** illustrates the phonon dispersion curves along the high-symmetry directions including Γ , Γ , and Z. Clearly, the overall values in **Figure 4** are positive and no virtual frequencies are observed in the full Brillouin zone. It is concluded that the rhombohedral phase structure of Y₂O₃:Ce crystal is dynamically stable.

Electronic Properties

To further elucidate the electronic properties of Y₂O₃:Ce crystal, we have performed a series of *ab initio* calculations including the

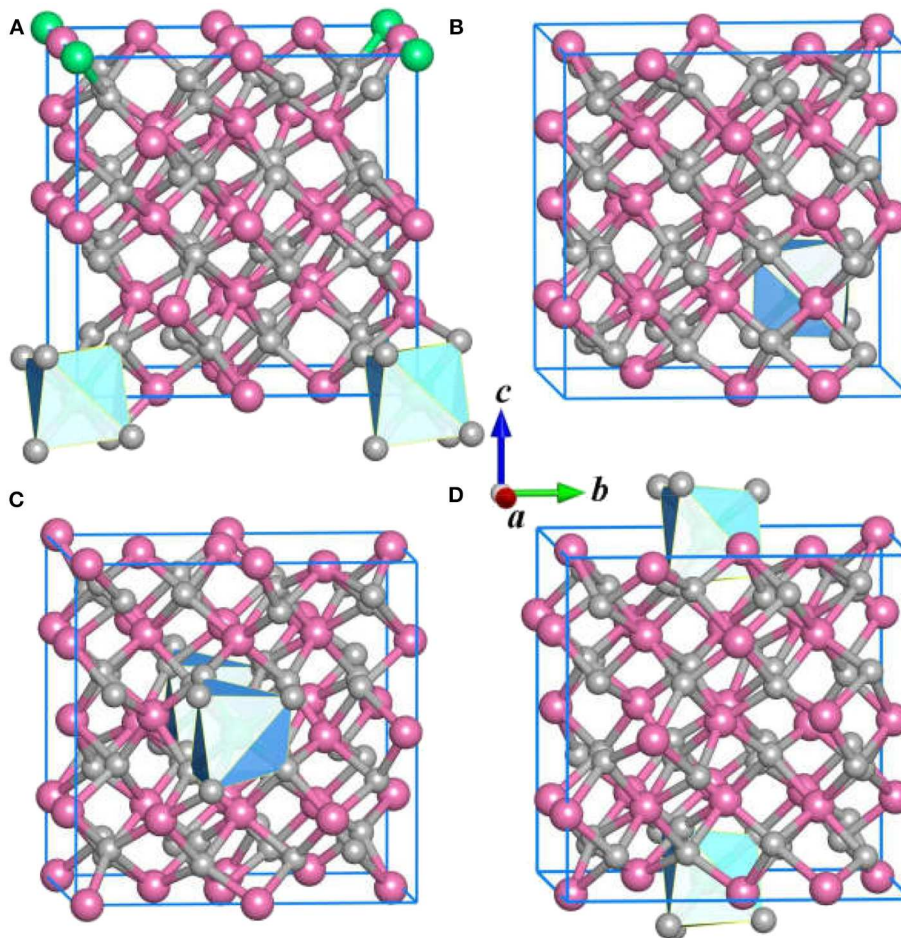
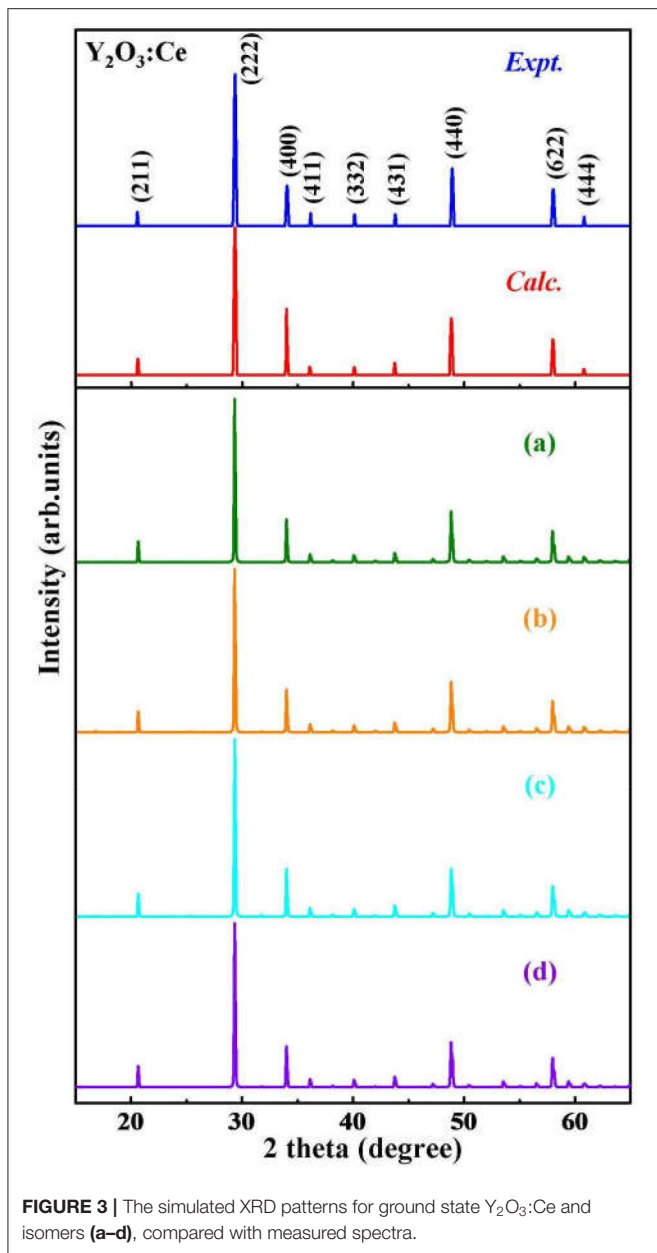


FIGURE 2 | The (A–D) isomers for Y₂O₃:Ce.

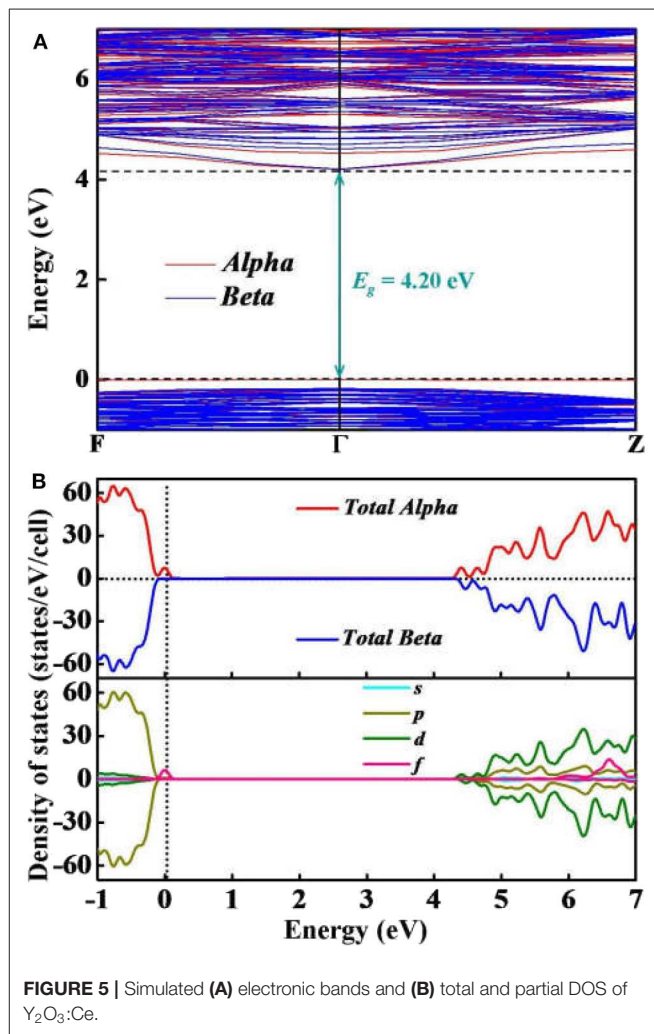
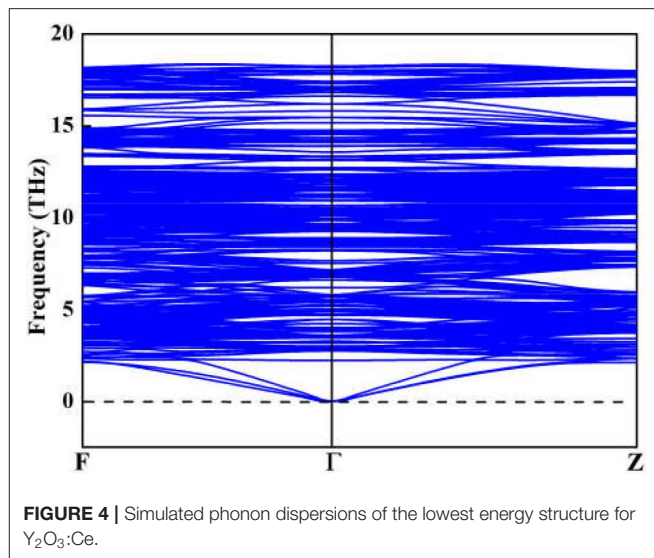
electronic band structures, total and partial electronic density of states and electron localization functions. The calculated band structure and density of states (DOS) are plotted together in **Figure 5**. Our calculated results show that both of the conduction band minimum and valence band maximum are identified at Γ site. The band structure is considered to be a typical of semiconductor with relatively flat top of the valence bands. According to the calculations, the band gap value of ground state Y₂O₃:Ce is equal to 4.20 eV directly at Γ point. This result is very close to the energy gap of Y₂O₃:Nd system (Ju et al., 2020) but significantly smaller than that of pure Y₂O₃ crystal (Wilk and Wallace, 2002). The direct band gap of 4.20 eV suggests a semiconductor character of the Y₂O₃:Ce. In addition to the electronic band gap, the electronic calculations of high-symmetry directions are in accordance with the above analysis based on phonon spectrum. In **Figure 5A**, we can clearly see that the band structures can be divided into three parts. The high conduction band is above 4.20 eV while the low valence band is below -0.17 eV. Interestingly, an extremely narrow valence band is observed just below the Fermi level. This result is greatly different with the band structures of pure Y₂O₃. The calculations show

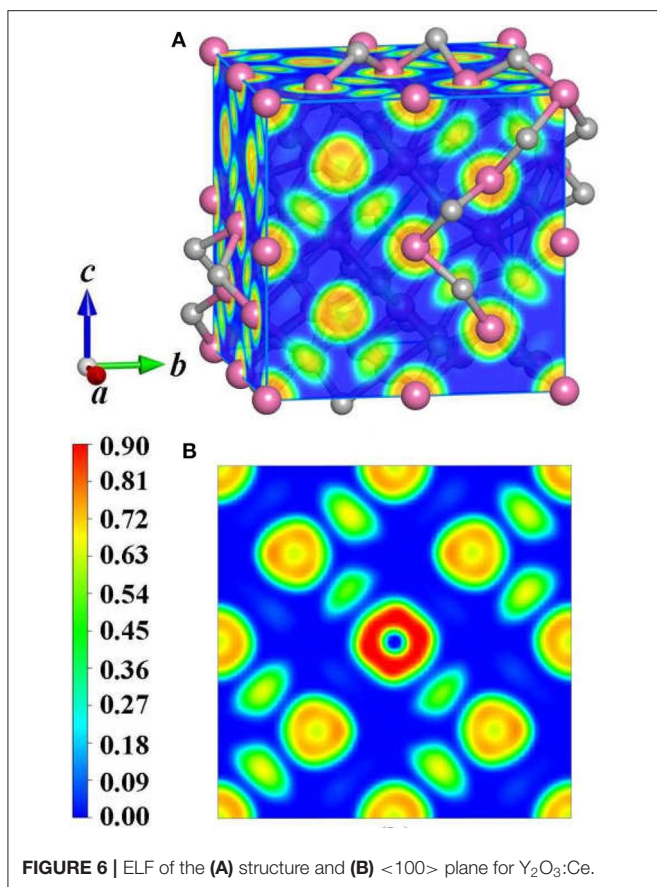
that the narrow valence band is caused by the electronic Alpha states. In contrast, the Beta electrons are not identified near the Fermi level. In order to explore the origins of the electronic bands, we further calculate the partial DOS including s, p, d and f states. The calculated DOS are depicted in **Figure 5B**. It can be clearly seen that the high conduction bands are mainly formed by d and p states. The p electrons are calculated to be the strongest state in the low valence bands. Moreover, the partial DOS of Y₂O₃:Ce reveals that the extremely narrow valence band near Fermi level is ascribed to the f orbital, which suggests that the impurity Ce³⁺ ion leads to a dramatic reduction of the band gap. In other words, it is concluded that the incorporation of the doped Ce³⁺ ion into Y₂O₃ host crystal results in an insulator to semiconductor transition.

To achieve foundational understanding of the bonding character and distribution of electrons of Y₂O₃:Ce crystal, we have carried out a calculation on the electron localization functions based on the ground state structure. The visually ELF of the structure and (100) plane are presented together in **Figure 6**. Obviously, the electrons near the cationic atoms are greatly localized with ELF values at ~ 0.9 while the ELF values



in the crystal lattice are nearly zero. This result indicates that the electrons localization on Ce and Y atoms broadens toward O atoms, forming a complete charge delocalization in the vicinity of O atoms. The strong ionic bonds are identified between Ce-O and Y-O. Furthermore, our calculations also show that the value of ELF at Ce atom is relatively larger than the ELF of Y atoms. This phenomenon can be explained as the remaining 4f (Masanori et al., 2020) electron of Ce³⁺ ion. It should be pointed out that there are strong charge localizations between O-O atoms, demonstrating the covalent bond of O atoms. To further quantitatively estimate the contribution of bonds between O atoms, we have presented the projected Crystal Orbital Hamilton

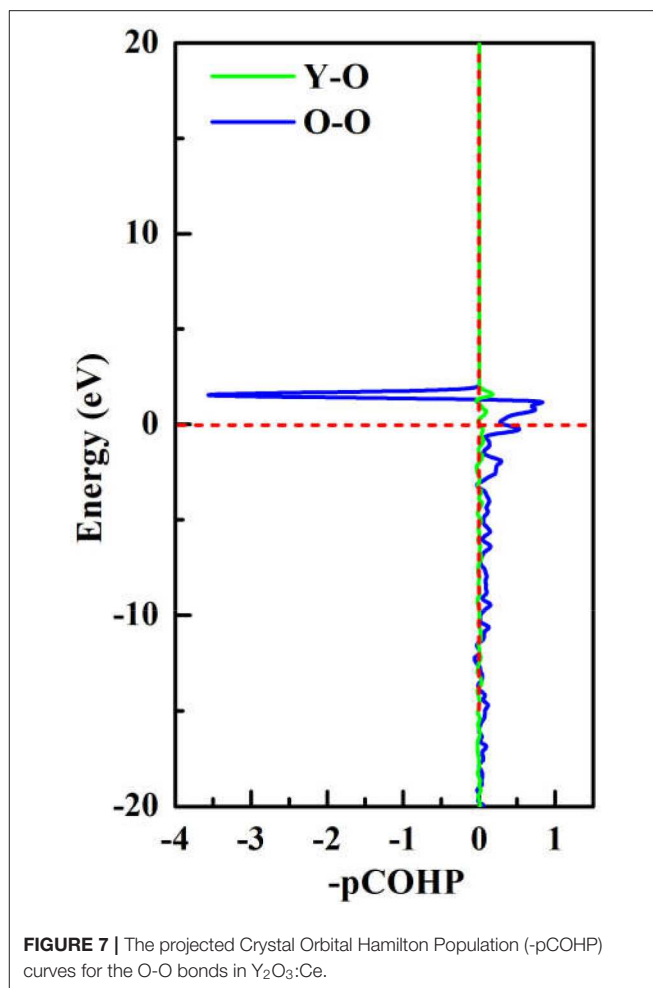




Population (-pCOHP) curves for the O-O bonds in Y₂O₃:Ce. As shown in **Figure 7**, the strong bonding contributions of O-O bonds are evidenced. The bond features near the Fermi level can be ascribed to covalent. It is convinced that the excellent stability of Y₂O₃:Ce crystal is owing to the strong covalent bonds of O atoms.

CONCLUSION

To summarize, we have systematically reported the structural evolutions, doping site locations and electronic properties of Y₂O₃ crystal doped with Ce³⁺ ions. By using the CALYPSO method in conjunction with first-principles calculations, a novel stable phase with R-3 space group is identified for the first time. For the ground state structure, the doped Ce³⁺ can naturally occupy the central Y³⁺ site in the crystal lattice of Y₂O₃, forming a standard cage-like structure. The cationic site symmetry of Ce³⁺ is calculated to be C_{3i} with six equal Ce-O bonds. The first four candidate isomers present different doping sites for Ce³⁺, which is helpful to investigate the structural evolution of Y₂O₃:Ce. By comparing the simulated XRD patterns with experimental data, we demonstrate the validity of the lowest energy structure. The dynamical stability of Y₂O₃:Ce crystal is carefully examined through the calculation of phonon dispersions. Our results of electronic band structures



reveal that both of the conduction band minimum and valence band maximum are located at Γ site, leading to a band gap value of 4.20 eV. This band gap suggests a semiconductor character of Y₂O₃:Ce system. Interestingly, an extremely narrow valence band near Fermi level is observed in the band structure and the contribution of this band is assigned to f orbital. In addition, the calculated results of visually ELF show that the charge localizations between O-O atoms are dramatically strong, suggesting the covalent bond character of O atoms in the Y₂O₃:Ce crystal. These findings could provide important information of the microstructures of rare-earth doped laser materials.

DATA AVAILABILITY STATEMENT

All datasets generated for this study are included in the article/supplementary material.

AUTHOR CONTRIBUTIONS

MJ, JW, and CZ conceived the idea. MJ, JH, YJ, YC, WS, and SL performed the calculations. MJ, JH,

and WS wrote the manuscript. All authors reviewed the manuscript.

FUNDING

This work was financial supported in part by National Natural Science Foundation of China (Nos. 11904297, 11747139,

and 11804031) and the Fundamental Research Funds for the Central Universities (SWU118055), the Scientific Research Project of Education Department of Hubei Province (No. Q20191301), the Open Research Projects of Wuhan Huada (No. NERCEL-OP2015001) and the Provincial Teaching Research Project in Hubei province of China (Grant No. 2017369).

REFERENCES

- Atsushi, T., Fumiyasu, O., and Isao, T. (1993). First-principles calculations of the ferroelastic transition between rutile-type and CaCl_2 -type SiO_2 at high pressures. *Phys. Rev. B* 78:134106.
- Becke, A. D., and Edgecombe, K. E. (1990). A simple measure of electron localization in atomic and molecular systems. *J. Chem. Phys.* 92, 5397–5403. doi: 10.1063/1.458517
- Chien, W. C., and Yu, Y. Y. (2008). Preparation of $\text{Y}_2\text{O}_3:\text{Ce}^{3+}$ phosphors by homogeneous precipitation inside bicontinuous cubic phase. *Mater. Lett.* 62, 4217–4219. doi: 10.1016/j.matlet.2008.06.041
- Gieszczyk, W., Bilski, P., Kłosowski, M., Mrozik, A., Zorenko, Yu., Zorenko, T., et al. (2019). Luminescent properties of undoped and Ce^{3+} doped crystals in $\text{Y}_2\text{O}_3\text{-Lu}_2\text{O}_3\text{-Al}_2\text{O}_3$ triple oxide system grown by micro-pulling-down method. *Opt. Mater.* 89, 408–413. doi: 10.1016/j.optmat.2019.01.023
- Han, Z. K., Zhang, L., Liu, M., Maria, V. G. P., and Gao, Y. (2019). The structure of oxygen vacancies in the near-surface of reduced CeO_2 (111) under strain. *Front. Chem.* 7:436. doi: 10.3389/fchem.2019.00795
- Herbst, J. F., and Waston, R. E. (1978). Relativistic calculations of 4f excitation energies in the rare-earth metals: further results. *Phys. Rev. B* 17, 3089–3098. doi: 10.1103/PhysRevB.17.3089
- Jia, W., Wang, Y., Fernandez, F., Wang, X., Huang, S., and Yen, W. M. (2001). Photoluminescence of $\text{Ce}^{3+}, \text{Tb}^{3+}:\text{Y}_2\text{O}_3$ nanoclusters embedded in SiO_2 sol-gel glasses. *Mater. Sci. Eng. C* 16, 55–58. doi: 10.1016/S0928-4931(01)00298-3
- Ju, M., Lu, C., Yeung, Y., Kuang, X., Wang, J., and Zhu, Y. (2016). Structural evolutions and crystal field characterizations of Tm-doped YAlO_3 : new theoretical insights. *ACS Appl. Mater. Interfaces* 8, 30422–30429. doi: 10.1021/acsami.6b09079
- Ju, M., Sun, G., Kuang, X., Lu, C., Zhu, Y., and Yeung, Y. (2017). Theoretical investigation of the electronic structure and luminescence properties for $\text{Nd}_x\text{Y}_{1-x}\text{Al}_3(\text{BO}_3)_4$ non-linear laser crystal. *J. Mater. Chem. C* 5, 7174–7181. doi: 10.1039/C7TC01911D
- Ju, M., Xiao, Y., Sun, W., Lu, C., and Yeung, Y. (2020). In-depth determination of the microstructure and energy transition mechanism for Nd^{3+} -doped yttrium oxide laser crystals. *J. Phys. Chem. C* 124, 2113–2119. doi: 10.1021/acs.jpcc.9b10482
- Ju, M., Xiao, Y., Zhong, M., Sun, W., Xia, X., Yeung, Y., et al. (2019b). New theoretical insights into the crystal-field splitting and transition mechanism for Nd^{3+} -doped $\text{Y}_3\text{Al}_5\text{O}_{12}$. *ACS Appl. Mater. Interfaces* 11, 10745–10750. doi: 10.1021/acsami.9b00973
- Ju, M., Zhong, M., Lu, C., and Yeung, Y. (2019a). Deciphering the microstructure and energy-level splitting of Tm^{3+} -doped yttrium aluminum garnet. *Inorg. Chem.* 58, 1058–1066. doi: 10.1021/acs.inorgchem.8b02009
- Kresse, G., and Furthmüller, J. (1996). Efficient iterative schemes for ab initio totalenergy calculations using a plane-wave basis set. *Phys. Rev. B* 54, 11169–11186. doi: 10.1103/PhysRevB.54.11169
- Kresse, G., and Hafner, J. (1993). Ab initio molecular dynamics for liquid metals. *Phys. Rev. B* 47, 558–561. doi: 10.1103/PhysRevB.47.558
- Krutikova, I., Ivanov, M., Murzakaev, A., and Nefedova, K. (2020). Laser-synthesized Ce^{3+} and Pr^{3+} doped Y_2O_3 nanoparticles and their characteristics. *Mater. Lett.* 265:127435. doi: 10.1016/j.matlet.2020.127435
- Kumar, P., Nagpal, K., and Gupta, B. K. (2017). Unclonable security codes designed from multicolour luminescent lanthanide doped Y_2O_3 nanorods for anti-counterfeiting. *ACS Appl. Mater. Interfaces* 9, 14301–14308. doi: 10.1021/acsami.7b03353
- Li, L., Hao, J., Liu, H., Li, Y., and Ma, Y. (2014). The metallization and superconductivity of dense hydrogen sulfide. *J. Chem. Phys.* 140:174712. doi: 10.1063/1.4874158
- Lin, Y. C., Bettinelli, M., and Karlsson, M. (2019). Unraveling the mechanisms of thermal quenching of luminescence in Ce^{3+} -doped garnet phosphors. *Chem. Mater.* 31, 3851–3862. doi: 10.1021/acs.chemmater.8b05300
- Liu, Y., Hu, S., Zhang, Y., Wang, Z., Zhou, G., and Wang, S. (2020). Crystal structure evolution and luminescence property of Ce^{3+} -doped $\text{Y}_2\text{O}_3\text{-Al}_2\text{O}_3\text{-Sc}_2\text{O}_3$ ternary ceramics. *J. Eur. Ceram. Soc.* 40, 840–846. doi: 10.1016/j.jeurceramsoc.2019.10.022
- Loitongbam, R. S., Singh, W. R., Phaomei, G., and Singh, N. S. (2013). Blue and green emission from Ce^{3+} and Tb^{3+} co-doped Y_2O_3 nanoparticles. *J. Lumin.* 140, 95–102. doi: 10.1016/j.jlumin.2013.02.049
- Lu, C., Amsler, M., and Chen, C. (2018). Unraveling the structure and bonding evolution of the newly discovered iron oxide FeO_2 . *Phys. Rev. B* 98:054102. doi: 10.1103/PhysRevB.98.054102
- Lu, C., and Chen, C. (2018). High-Pressure evolution of crystal bonding structures and properties of FeOOH . *J. Phys. Chem. Lett.* 9, 2181–2185. doi: 10.1021/acs.jpclett.8b00947
- Lu, C., Li, Q., Ma, Y., and Chen, C. (2017). Extraordinary indentation strain stiffening produces superhard tungsten nitrides. *Phys. Rev. Lett.* 119:11550. doi: 10.1103/PhysRevLett.119.115503
- Lu, C., Miao, M., and Ma, Y. (2013). Structural evolution of carbon dioxide under high pressure. *J. Am. Chem. Soc.* 135, 14167–14171. doi: 10.1021/ja404854x
- Lupei, A., Lupei, V., and Hau, S. (2017). Vibronics in optical spectra of Yb^{3+} and Ce^{3+} in YAG and Y_2O_3 ceramics. *Opt. Mater.* 63, 143–152. doi: 10.1016/j.optmat.2016.06.024
- Marin, R., Back, M., Mazzucco, N., Enrichi, F., Frattini, R., Benedetti, A., et al. (2013). Unexpected optical activity of cerium in $\text{Y}_2\text{O}_3:\text{Ce}^{3+}, \text{Yb}^{3+}, \text{Er}^{3+}$ up and down-conversion system. *Dalton Trans.* 42, 16837–16845. doi: 10.1039/C3DT51297E
- Masanori, N., Akira, M., Daisuke, U., Yuki, M., Yosuke, G., Yoshikazu, M., et al. (2020). Flux growth and superconducting properties of $(\text{Ce}, \text{Pr})\text{OBI}_2\text{S}_2$ single crystals. *Front. Chem.* 8:44. doi: 10.3389/fchem.2020.00044
- Ming, C., Pei, M., Ren, X., Xie, N., Cai, Y., Qin, Y., et al. (2018). Improving luminescent penetrability by $\text{Tm}^{3+}/\text{Ce}^{3+}$ doped Y_2O_3 nanocrystals for optical imaging. *Mater. Lett.* 218, 154–156. doi: 10.1016/j.matlet.2018.01.169
- Momma, K., and Izumi, F. (2011). VESTA 3 for three-dimensional visualization of crystal, volumetric and morphology data. *J. Appl. Crystallogr.* 44, 1272–1276. doi: 10.1107/S0021889811038970
- Perdew, J. P., Burke, K., and Ernzerhof, M. (1996). Generalized gradient approximation made simple. *Phys. Rev. Lett.* 77, 3865–3868. doi: 10.1103/PhysRevLett.77.3865
- Richard, D., and Peter, E. B. (1993). Crystal Orbital Hamilton Populations (COHP). Energy-resolved visualization of chemical bonding in solids based on density-functional calculations. *J. Phys. Chem.* 97, 8617–8624. doi: 10.1021/j100135a014
- Savin, A., Jepsen, O., Flad, J., Andersen, O. K., Preuss, H., and von Schnering, H. G. (1992). Electron localization in solid-state structures of the elements: the diamond structure. *Angew. Chem. Int. Ed. Engl.* 31, 187–188. doi: 10.1002/anie.199201871
- Stefan, M., Volker, L. D., Andrei, L. T., and Richard, D. (2016). LOBSTER: a tool to extract chemical bonding from plane-wave based DFT. *J. Comput. Chem.* 37, 1030–1035. doi: 10.1002/jcc.24300
- Taibeche, M., Guerbous, L., Boukerika, A., Kechouane, M., Nedjar, R., and Zergoug, T. (2016). Ab-initio simulations at the atomic scale of an exceptional

- experimental photoluminescence signal observed in Ce³⁺-doped Y₂O₃ sesquioxide system. *Opt.* 127, 10561–10568. doi: 10.1016/j.ijleo.2016.08.092
- Volker, L. D., Andrei, L. T., and Richard, D. (2011). Crystal Orbital Hamilton Population (COHP) analysis as projected from plane-wave basis sets. *J. Phys. Chem. A* 115, 5461–5466. doi: 10.1021/jp202489s
- Wang, N., He, J., Ye, K., Song, X., and L, T. (2018). Sol-gel synthesis and enhanced 1.54 μm emission in Y₂O₃:Yb³⁺, Er³⁺ nanophosphors co-doped with Ce³⁺ ions. *Infrared Phys. Technol.* 93, 77–80. doi: 10.1016/j.infrared.2018.07.023
- Wang, Y., Lv, J., Zhu, L., and Ma, Y. (2010). Crystal structure prediction via particleswarm optimization. *Phys. Rev. B* 82:094116. doi: 10.1103/PhysRevB.82.094116
- Wang, Y., Lv, J., Zhu, L., and Ma, Y. (2012). CALYPSO: a method for crystal structure prediction. *Comput. Phys. Commun.* 183, 2063–2070. doi: 10.1016/j.cpc.2012.05.008
- Wilk, G., and Wallace, R. M. (2002). Alternative gate dielectrics for microelectronics. *Mater. Res. Soc. Bull.* 27:3. doi: 10.1557/mrs2002.70
- Zhu, L., Wang, X., Yu, G., Hou, X., Zhang, G., Sun, J., et al. (2008). Effect of Ce³⁺ doping and calcination on the photoluminescence of ZrO₂ (3% Y₂O₃) fibers. *Mater. Res. Bull.* 43, 1032–1037. doi: 10.1016/j.materresbull.2007.04.025

Conflict of Interest: The authors declare that the research was conducted in the absence of any commercial or financial relationships that could be construed as a potential conflict of interest.

Copyright © 2020 Ju, Wang, Huang, Zhang, Jin, Sun, Li and Chen. This is an open-access article distributed under the terms of the Creative Commons Attribution License (CC BY). The use, distribution or reproduction in other forums is permitted, provided the original author(s) and the copyright owner(s) are credited and that the original publication in this journal is cited, in accordance with accepted academic practice. No use, distribution or reproduction is permitted which does not comply with these terms.